Department of AERONAUTICS and ASTRONAUTICS
STANFORD UNIVERSITY

S.C. McINTOSH, JR.
T.A. WEISSHAAR
H. ASHLEY

PROGRESS IN AEROELASTIC OPTIMIZATION — ANALYTICAL VERSUS NUMERICAL APPROACHES

Supported by the Air Force Office of Scientific
Research under Contract No. F 44620-68-C-0036
and the National Aeronautics and Space Administration
under Grants NGR 05-020-102 and NGR 05-020-243

JULY
1969

SUDAAR
NO. 383

Department of Aeronautics and Astronautics
Stanford University
Stanford, California

PROGRESS IN AEROELASTIC OPTIMIZATION - ANALYTICAL VERSUS NUMERICAL APPROACHES

by

S. C. McIntosh, Jr.

T. A. Weisshaar

H. Ashley

SUDAAR NO. 383

July 1969

Presented at the AIAA Structural Dynamics and Aeroelasticity Specialist Conference, New Orleans, April 1969

Supported by the Air Force Office of Scientific Research under Contract No. F 44620-68-C-0036 and the National Aeronautics and Space Administration under Grants NGR 05-020-102 and NGR 05-020-243

ACKNOWLEDGMENTS

This work was carried out as part of a research program sponsored by the Air Force Office of Scientific Research and the National Aeronautics and Space Administration. Valuable assistance was also provided by Mr. Jean-Louis Armand.

ABSTRACT

A summary is given of recent developments in aeroelastic optimization, with emphasis on difficulties encountered in treating examples numerically by adaptation of techniques from optimal control theory. The elementary problem of finding the unswept wing of least skin mass for fixed torsional divergence speed is used to show how a numerical transition-matrix solution is easily obtained that reproduces accurately the analytical solution. Other problems are then considered to illustrate the application of transition-matrix or gradient methods where solutions are not so easily found. One such problem is to determine the minimum-mass skin thickness distribution of an unswept wing with fixed pure-torsional flutter speed and frequency. In this case the analytical treatment reveals that only certain ranges of the system parameters will allow a physically meaningful solution. Other problems of more practical importance, such as the minimum-weight sandwich panel for fixed flutter eigenvalues and the minimum-weight unswept wing for fixed speed and frequency of bending-torsion flutter, are treated in various ways. An attempt is made to identify those methods most likely to be successful and to outline some of the difficulties involved in applying them to aeroelastic optimization.

TABLE OF CONTENTS

NOMENCLATURE

a_m	Modal amplitude - see Eqs. (44)
AR	Aspect ratio, L/2B for rectangular wing
b_m	Modal amplitude - see Eqs. (44)
B	Dimensional wing semichord
c_p	Modal amplitude - see Eqs. (44)
C	Dimensional panel chord
d	Dimensionless distance between elastic axis and line of centers of gravity, D/B
d_p	Modal amplitude - see Eqs. (44)
D	Dimensional distance between elastic axis and line of centers of gravity, positive for c. g. line aft of e. a.
D_p	Sandwich panel stiffness parameter, $EH^2T(X)/4(1 - \nu^2)$ (E here is Young's modulus)
D_0	Stiffness parameter for uniform or constant-thickness sandwich panel, $ET_0^3/12(1 - \nu^2)$ or $EH^2T_0/4(1 - \nu^2)$ (E here is Young's modulus)
e	Dimensionless distance between elastic axis and line of aerodynamic centers, E/B
E	Dimensional distance between elastic axis and line of aerodynamic centers, positive for a. c. line forward of e. a.
EI	Flexural rigidity
F	Euler-Lagrange functional
GJ	Torsional rigidity
H	Dimensional panel core depth
I_α	Section mass moment of inertia about elastic axis

k	Reduced frequency, $\omega B/V$
$\overline{K}$	Dimensionless panel parameter, $M_0 C^4 \omega^2/D_0 - i\lambda_0(\omega C/V)(M_\infty^2-2)/(M_\infty^2-1)$
K_0	Dimensionless panel reference parameter, $M_0 C^4 \omega^2/D_0$
L	Wing semispan
L_α, L_h	Dimensionless oscillatory aerodynamic lift coefficients - see Ref. 13
L_Y	Section lift, positive upward
m	Ratio of optimized mass to reference mass - see Eq. (1) or Eq. (26)
M	Dimensional panel or wing mass distribution
M_α, M_h	Dimensionless oscillatory aerodynamic moment coefficients - see Ref. 13
M_X	Section pitching moment about elastic axis, positive nose up
M_∞	Free-stream Mach number
N_x	Dimensional panel in-plane load
p	Intermediate physical variable - see Eqs. (14)
q	Intermediate physical variable - see Eqs. (14)
q_∞	Free-stream dynamic pressure, $\rho_\infty V^2/2$
r	Intermediate physical variable - see Eqs. (14)
r_α	Dimensionless section radius of gyration, $(I_\alpha/MB^2)^{1/2}$
R_x	Dimensionless panel in-plane load, $N_x C^2/D_0$
s	Intermediate physical variable - see Eqs. (14)
S_α	Section static unbalance, MD
t	Dimensionless thickness distribution, T/T_0
t_n	Modal amplitude for thickness distribution
T	Dimensional thickness distribution
V	Free-stream speed

w	Dimensionless amplitude of panel displacement -- $\tilde{w}(x, \tau) = w(x)e^{i\omega\tau}$
$\tilde{w}$	Dimensionless panel displacement , W/C
W	Dimensional panel midsurface displacement
x	Dimensionless space coordinate -- X/L for wing, X/C for panel
X	Dimensional space coordinate - spanwise for wing, chordwise for panel
y	Dimensionless amplitude of section elastic-axis displacement -- $Y(X, \tau) = \bar{y}(x)e^{i\omega\tau}$
y_n	Modal amplitude for y
Y	Dimensional section elastic-axis displacement, positive downward
$\alpha, \alpha_1, \alpha_2, \beta, \beta_1, \beta_2, \gamma_1, \gamma_2, \delta_1, \delta_2$	Dimensionless parameters for wing and panel - see Eqs. (9) and Eqs.(38)
η	Fraction of total mass effective structurally
θ	Amplitude of section rotation -- $\Theta(X,\tau) = \bar{\theta}(x)e^{iw\tau}$
θ_n	Modal amplitude for θ
Θ	Section rotation, positive nose up
$\lambda_i, \lambda_p, \lambda_q, \lambda_r, \lambda_s, \lambda_y, \lambda_\theta, \lambda_w$	Lagrange multipliers or adjoint variables
λ_0	Panel dynamic-pressure parameter, $2q_\infty C^3/D_0(M_\infty^2 - 1)^{1/2}$
μ	Panel-air mass ratio, $M_0/\pi\rho_\infty B^2$
ν	Poisson's ratio
ρ_∞	Free-stream mass density
τ	Dimensional time
ω	Frequency

ω_y	Reference bending frequency, $(EI_0/M_0L^4)^{1/2}$
ω_θ	Reference torsional frequency, $(GJ_0/I_{\alpha_0}L^2)^{1/2}$

Subscripts

$(\ )_0$	Quantities for reference system--system with uniform thickness and same aeroelastic eigenvalues as optimized system

Superscripts

$\bar{(\ )}$	Complex quantities
$(\ )'$	Differentation with respect to x

I. INTRODUCTION; SURVEY OF PREVIOUS WORK

The introduction of stiffness constraints, and in particular truly aeroelastic constraints, into the weight optimization of structures has a relatively recent history. The earliest examples of this work known to the authors are a series of reports by Lunn and others and Hodson, Refs. 1-3. A formal optimization process such as that described herein was not used, but in its stead those investigators used some very insightful intuitive criteria, such as the requirement of uniform torsional stress throughout the structure for optimality (minimum structural weight) at divergence. Schmit and Thornton[4] imposed a lower bound on the flutter speed, among a number of other constraints, in their synthesis of an airfoil for minimum total drag work. The merit function is different, but this analysis is a good illustration of the sophistication that can be achieved for more realistic situations where multiple constraints are necessary. The first published paper with a constraint on a natural frequency was apparently that of Niordson[5]; this approach was continued by Taylor[6] and Prager and Taylor[7], who studied a wide class of both static and dynamic problems and presented important proofs of uniqueness and optimality in certain cases. Taylor[7] also suggested that in many instances it may be profitable to interchange the roles of the constraint eigenvalue and the merit function. For example, the minimum-weight bar for fixed lowest natural frequency of axial vibration can be found in two ways: one can maximize the frequency for fixed total mass, or one can minimize the mass for fixed frequency. The latter approach was followed by

Turner[8,9], who also introduced for the first time a distinctly aeroelastic constraint into a minimum-weight problem.

It is possible to distinguish two different approaches toward aeroelastic optimization:

(1) The structure is idealized and its degrees of freedom limited by the use of, say, finite-element techniques, so that one is led naturally to the solution of algebraic equations. Turner's papers[8,9] are representative of this point of view, for which the motivation is to achieve the capability of treating complex built-up structures representative of actual design. It goes without saying that any sort of aeroelastic optimization procedure for use in the design of actual hardware must make use of such approximate techniques.

(2) Simplified (and therefore less realistic) structures are examined, so that the solutions may be found by differential-equation methods. This search for solutions in function space will, it is believed, make it possible to explore to the fullest the potentials of aeroelastic optimization and to seek results of general applicability. It is also emphasized that there are as yet many important theoretical questions, such as that concerning uniqueness for problems with dynamic aeroelastic constraints, that remain unanswered. These certainly merit further study in connection with elementary examples whose mathematical description is not too complicated.

The formulation of the problem is next discussed in a general way. The figure of merit will in all cases be weight, expressed as an appropriate integral of some material thickness distribution, but there is no reason that other mass-related figures of merit, such as total moment of inertia, could not be taken instead. An appropriate relation is found between the thickness distribution and the stiffness distribution, so that the latter's dependence on thickness appears explicitly.

Reference quantities for the corresponding uniform-thickness system with the same aeroelastic eigenvalue are used to render all variables dimensionless. Thus, for example, if the optimum thickness distribution T(X) is made dimensionless by division by the skin thickness T_0 of the aforementioned reference system, the ratio of the optimized weight to the reference weight is simply

$$m = \int_0^L [T(X)/LT_0]dX = \int_0^1 t(x)dx \tag{1}$$

where $X = Lx$. The constraint equations are the appropriate aeroelastic equations, organized into an equivalent system of first-order ordinary differential equations:

$$q_i' - f_i(q_1, \ldots, q_N, t) = 0, \quad i = 1, 2, \ldots, N \tag{2}$$

The $q_i(x)$ represents the N dependent variables along with the unknown thickness distribution t(x), x being a spatial coordinate measuring distance along the one-dimensional structure. The dependence of the equations on time has been eliminated, if appropriate, by the usual assumption of simple harmonic

motion. A functional is formed, consisting of the thickness distribution to be optimized augmented by Lagrange multipliers $\lambda_i(x)$ factoring in the constraint equations:

$$F = t + \sum_{i=1}^{N} \lambda_i (f_i - q_i') \tag{3}$$

Conditions for an extremum of this functional are given by the Euler-Lagrange equations:

$$\begin{aligned} &\frac{d}{dx}\left(\frac{\partial F}{\partial q_i'}\right) - \frac{\partial F}{\partial q_i} = 0, \quad i = 1, 2, \ldots, N \\ &\frac{d}{dx}\left(\frac{\partial F}{\partial t'}\right) - \frac{\partial F}{\partial t} = 0 \end{aligned} \tag{4}$$

There are therefore 2N+1 unknowns -- the N q_i, the N λ_i, and t -- and 2N+1 equations -- the N+1 Euler-Lagrange equations plus the N constraint equations. Boundary conditions are provided for the physical variables q_i by the manner in which the system is restrained at its extremities and for the adjoint variables λ_i by the transversality conditions[10]. The equations are nonlinear, involving products or quotients of t and certain of the q_i or λ_i. In addition, the problem is a two-point boundary-value problem. It is therefore usually too complicated to solve analytically, except in certain simple cases, so that a numerical iteration scheme must be employed. In general, there is no a priori guarantee that a physically meaningful solution exists, nor is there any assurance that an optimal solution, once found, is the absolute optimum. In light of these considerations, it was speculated that some of the numerical techniques of optimal control theory (as described in Ref. 11, for example) might be readily adapted to the solution of such problems. Subsequent sections of this paper will

describe applications of these techniques to several problems involving both static and dynamic aeroelastic constraints.

II. A STATIC AEROELASTIC CONSTRAINT: TORSIONAL DIVERGENCE

A simple problem that has the virtue of possessing an analytical solution for comparison with numerical results is that of finding the unswept cantilever wing, of rectilinear or straight-tapered planform, with the least skin weight for fixed torsional divergence speed. Such a wing is illustrated in Fig. 1. The planform and airfoil section are fixed, and the torsional stiffness is assumed to be dominated by contributions from a thin outer skin of thickness T(x). The equations resulting from an optimization scheme as described in Sect. I are easily solved analytically and yield for a wing of rectilinear planform the skin thickness distribution shown in Fig. 2, which is reproduced from Ref. 12. The skin thickness T(x) has been rendered dimensionless by division by the skin thickness T_0 of a constant-thickness wing with the same planform and divergence speed, so on the plot of Fig. 2 t = 1.0 represents the distribution of the reference wing. The skin weight of the "optimum" wing is 82% of that of the reference wing. Superimposed on the analytically derived curve are points calculated numerically by a transition-matrix procedure (Ref. II, Sect. 7.3). This procedure will be discussed in more detail in Sect. III; here it is sufficient to note that one encountered virtually no difficulties in applying it. After some 15 iterations beyond the initial estimate of the unknown boundary conditions at the root, the numerical solution reproduced the analytical solution extremely accurately. The initial guesses were varied to test the sensitivity of the procedure to their inaccuracies. Although an exhaustive study was not made, it did appear that the solution process was relatively insensitive to these variations, in the sense that a fairly naive initial guess could be made without confounding the procedure.

III. A DYNAMIC AEROELASTIC CONSTRAINT: BENDING-TORSION FLUTTER

Another problem which has received considerable attention involves finding the unswept cantilever rectangular wing of least skin weight for fixed speed (or speed and frequency) of bending-torsion flutter. The notation is shown in Fig. 3. The equations of motion for this wing, treated as a beam with infinite chordwise rigidity, can be written as follows:

$$\frac{\partial^2}{\partial X^2}\left(EI\frac{\partial^2 Y}{\partial X^2}\right) + M\frac{\partial^2 Y}{\partial \tau^2} + S_\alpha \frac{\partial^2 \Theta}{\partial \tau^2} = L_Y(X,\tau)$$

$$\frac{\partial}{\partial X}\left(GJ\frac{\partial \Theta}{\partial X}\right) - I_\alpha \frac{\partial^2 \Theta}{\partial \tau^2} - S_\alpha \frac{\partial^2 Y}{\partial \tau^2} = -M_X(X,\tau) \qquad (5)$$

The aerodynamic loading is decomposed into a section lift $L_Y(X,\tau)$, positive upward, and a section pitching moment $M_X(X,\tau)$, positive nose up. With the assumption of simple harmonic motion and the use of incompressible strip theory for the aerodynamic loads, L_Y and M_X can be written as functions of the air density, speed, frequency, semichord B, elastic-axis offset E, and the amplitudes of the motion, as described, for example, in Ref. 13. It is also assumed that EI(X) and GJ(X) are determined primarily by the sectional skin thickness T(X) and are in fact proportional to it. Finally, it is supposed for present purposes that the mass associated with the skin is the dominant part of the total section mass, so that M(X) is also proportional to T(X). With the zero subscript denoting the properties of the reference wing, the proportionality

assumptions can be written as

$$EI(X) = EI_0 t(X)$$

$$GJ(X) = GJ_0 t(X) \tag{6}$$

$$M(X) = M_0 t(X)$$

where

$$t(X) = T(X)/T_0 \tag{7}$$

Simple harmonic motion is now assumed, so that $Y(X,\tau) = L\bar{y}(x)e^{i\omega\tau}$, $\Theta(X,\tau) = \bar{\theta}(x)e^{i\omega\tau}$. Bars are placed over complex quantities, and primes denote differentiation with respect to $x = X/L$. With the time dependence canceled out after nondimensionalization, Eqs. (5) become

$$\begin{aligned}
&(t\bar{y}'')'' - (\alpha_1 t + \bar{\alpha}_2)\,\bar{y} - (\beta_1 t + \bar{\beta}_2)\,\bar{\theta} = 0 \\
&(t\bar{\theta}')' + (\gamma_1 t + \bar{\gamma}_2)\,\bar{y} + (\delta_1 t + \bar{\delta}_2)\,\bar{\theta} = 0
\end{aligned} \tag{8}$$

where

$$\begin{aligned}
&\alpha_1 = (\omega/\omega_y)^2,\ \bar{\alpha}_2 = (\omega/\omega_y)^2\,\bar{L}_h/\mu, \\
&\beta_1 = dAR(\omega/\omega_y)^2,\ \bar{\beta}_2 = (\omega/\omega_y)^2\,(\bar{L}_\alpha - e\bar{L}_h)/\mu r_\alpha^2, \\
&\gamma_1 = dAR\,(\omega/\omega_\theta)^2/r_\alpha^2,\ \bar{\gamma}_2 = AR\,(\omega/\omega_\theta)^2\,(M_h - e\bar{L}_h)/\mu r_\alpha^2, \\
&\delta_1 = (\omega/\omega_\theta)^2,\ \bar{\delta}_2 = (\omega/\omega_\theta)^2\,[\bar{M}_\alpha - e(\bar{L}_\alpha + M_h) + e^2\bar{L}_h]/\mu r_\alpha^2
\end{aligned} \tag{9}$$

The quantities $\bar{L}_h$, $\bar{L}_\alpha$, M_h, and $\bar{M}_\alpha$ are tabulated functions of reduced frequency $k = \omega B/V$.[13] The other parameters appearing in Eqs. (9) are functions of airstream and reference-wing properties as defined in the Nomenclature.

Boundary conditions are those appropriate for a cantilever root,

$$\bar{y} = \bar{y}' = \bar{\theta} = 0, \quad x = 0 \tag{10}$$

and for a free tip,

$$t\bar{y}'' = (t\bar{y}'')' = t\bar{\theta}' = 0, \quad x = 1 \tag{11}$$

To obtain the equations that must be satisfied for an optimal solution, one forms a functional F incorporating as constraints Eqs. (8), written in expanded form as outlined in Sect. I. Since these relations are complex, however, the functional must be modified slightly to assure that t(x) remains real. The Euler-Lagrange equations are therefore written for a functional defined as follows:[9]

$$\begin{aligned} F = t + \mathrm{Re}\Big\{ & \bar{\lambda}_y(\bar{p} - \bar{y}') + \bar{\lambda}_p(\bar{q}^*/t - \bar{p}') \\ & + \bar{\lambda}_q(\bar{r} - \bar{q}') + \bar{\lambda}_r[(\alpha_1 t + \bar{\alpha}_2)\bar{y} + (\beta_1 t + \bar{\beta}_2)\bar{\theta} - \bar{r}'] \\ & + \bar{\lambda}_\theta(\bar{s}/t - \bar{\theta}') + \bar{\lambda}_s[-(\gamma_1 t + \bar{\gamma}_2)\bar{y} - (\delta_1 t + \bar{\delta}_2)\bar{\theta} - \bar{s}'] \Big\} \end{aligned} \tag{12}$$

That is, one appends to the unconstrained merit function t(x) the real part of the products of the complex Lagrange multipliers, or adjoint variables, and the expanded constraint equations. Applying Eqs. (4) to F as defined above, with the q_i now representing the real and imaginary parts of $\bar{p}$, $\bar{q}$, $\bar{r}$, $\bar{y}$, $\bar{s}$, and $\bar{\theta}$, produces 13 Euler-Lagrange equations. These can be written in compact form as

$$\bar{\lambda}_y' = -(\alpha_1 t + \bar{\alpha}_2)\bar{\lambda}_r + (\gamma_1 t + \bar{\gamma}_2)\bar{\lambda}_s$$

$$\bar{\lambda}_p' = -\bar{\lambda}_y$$

(continued)

$$\bar{\lambda}_q' = -\bar{\lambda}_p/t$$

$$\bar{\lambda}_r' = -\bar{\lambda}_q$$

$$\bar{\lambda}_\theta' = -(\beta_1 t + \bar{\beta}_2)\bar{\lambda}_r + (\delta_1 t + \bar{\delta}_2)\bar{\lambda}_s \qquad (13)$$

$$\bar{\lambda}_s' = -\bar{\lambda}_\theta/t$$

$$\mathrm{Re}\left\{\bar{\lambda}_p \bar{q}/t^2 - \bar{\lambda}_r(\alpha_1\bar{y} + \beta_1\bar{\theta}) + \bar{\lambda}_\theta \bar{s}/t^2 + \bar{\lambda}_s(\gamma_1\bar{y} + \delta_1\bar{\theta})\right\} = 1$$

It is interesting to note that forming an F so that t(x) remains real, as in Eq. (12), affects only the control equation (the last of Eqs. (13) above). With that exception, Eqs. (13) are the same as those that would be found from a complex F.

The system of equations is completed by the constraint equations, 12 in all:

$$\bar{y}' = \bar{p}$$

$$\bar{p}' = \bar{q}/t$$

$$\bar{q}' = \bar{r}$$

$$\bar{r}' = (\alpha_1 t + \bar{\alpha}_2)\bar{y} + (\beta_1 t + \bar{\beta}_2)\bar{\theta} \qquad (14)$$

$$\bar{\theta}' = \bar{s}/t$$

$$\bar{s}' = -(\gamma_1 t + \bar{\gamma}_2)\bar{y} - (\delta_1 t + \bar{\delta}_2)\bar{\theta}$$

The physical boundary conditions become (cf. Eqs. (10)-(11))

$$\bar{y} = \bar{p} = \bar{\theta} = 0, \quad x = 0$$
$$\qquad (15)$$
$$\bar{q} = \bar{r} = \bar{s} = 0, \quad x = 1$$

The remaining boundary conditions are given by the transversality condition, which in this case merely requires that the Lagrange multipliers corresponding

to the physical variables unspecified at the boundaries be zero:

$$\bar{\lambda}_q = \bar{\lambda}_r = \bar{\lambda}_s = 0, \quad x = 0$$

$$\bar{\lambda}_y = \bar{\lambda}_p = \bar{\lambda}_0 = 0, \quad x = 1 \tag{16}$$

The transition-matrix algorithm was then attempted with Eqs. (13)-(14), subject to the boundary conditions, Eqs. (15)-(16). The algorithm proceeds as follows:*

(a) Along with the 12 known variables at x = 0, estimate starting values for the other 12 that are not known - the complex values of $\bar{q}(0)$, $\bar{r}(0)$, $\bar{s}(0)$, $\bar{\lambda}_y(0)$, $\bar{\lambda}_p(0)$, $\bar{\lambda}_\theta(0)$. The control equation gives a starting value for t, since it can be rewritten to give t algebraically as a function of the other dependent variables.

(b) Integrate the 24 differential equations, Eqs. (13)-(14), from x = 0 to x = 1, using the control equation to calculate t as the integration proceeds. Record the final values of the variables that are specified at x = 1 - $\bar{q}(1)$, $\bar{r}(1)$, $\bar{s}(1)$, $\bar{\lambda}_y(1)$, $\bar{\lambda}_p(1)$, $\bar{\lambda}_\theta(1)$. These, in general, will not be the values desired.

---

*It is remarked that no solution has yet been obtained for the bending-torsion flutter problem by the procedure here detailed. It is, however, included for two reasons. First, it did form the basis for successful examples reported in Ref. 12. Second, the authors are confident that, with refined means for establishing initial estimates and other such improvements, the transition matrix will prove the most efficient route to solution of differential-equation systems of the type encountered here.

(c) Estimate the partial derivatives $\partial\overline{q}(1)/\partial\overline{q}(0)$, $\partial\overline{r}(1)/\partial\overline{q}(0)$, etc., by incrementing in turn by small amounts one and only one of the 12 guessed initial values, integrating the equations each time over the span, and dividing the changes in the final values by the increment in the initial value. These integrations are performed a total of 12 times. Each integration with one increment will give a column of partial derivatives, and therefore a 12 x 12 matrix is filled column by column. For example, the first column might be the partial derivatives of the 12 final values with respect to the real part of $\overline{q}(0)$, the second column might be the derivatives with respect to the imaginary part of $\overline{q}(0)$, and so on. Let this matrix be called [TR] and let $\{Q_I\}$ and $\{Q_F\}$ denote column matrices of, respectively, the values of the variables unspecified at x = 0 and the current values of the variables specified at x = 1. Then, in a small neighborhood of the solution just found with the initial guess for $\{Q_I\}$, one adopts the approximation

$$\{\Delta Q_F\} \simeq [TR] \{\Delta Q_I\} \tag{17}$$

(d) Calculate the desired changes in the current final values as

$$\{\Delta Q_F\} = -\epsilon \{Q_F\} \tag{18}$$

Here ϵ is a positive number between zero and unity, which determines in effect how great a step towards the solution is

to be taken for the next iteration. The changes in the initial values necessary to achieve this step are approximated by

$$\left\{\Delta Q_I\right\} \simeq [TR]^{-1} \left\{\Delta Q_F\right\} \tag{19}$$

with $\left\{\Delta Q_F\right\}$ given from Eq. (18).

(e) The first guess for the initial values is incremented by $\left\{\Delta Q_I\right\}$, and the algorithm is repeated until the calculated final values approximate those desired to an appropriate degree of accuracy.

The reference wing chosen for the calculations was one tested and analyzed by Runyan and Watkins (Ref. 14), from which are found the parameters $k = 0.159$, $(\omega/\omega_y)^2 = 179.1$, $(\omega/\omega_\theta)^2 = 0.673$, $d = 0.039$, $AR = 12$, $e = 0.374$, $\mu = 32.6$, $r_\alpha^2 = 0.266$. From these values plus the aerodynamic loads of Ref. 13 for $k = 0.159$, the parameters used in the calculation become $\alpha_1 = 179.1$, $\bar{\alpha}_2 = -7.456 - 52.77i$, $\beta_1 = 83.82$, $\bar{\beta}_2 = -28.36 + 1.167i$, $\gamma_1 = 1.184$, $\bar{\gamma}_2 = 0.9386 + 3.347i$, $\delta_1 = 0.6730$, $\bar{\delta}_2 = 1.813 - 0.5629i$.

Lacking any means of making an informed first guess for the 12 unknown boundary conditions at one end, the first author encountered numerical problems in attempting this procedure. As can be seen from the control equation, the last of Eqs. (13), solving for the thickness t at any step in the integration of the differential equations involves a radical, the argument of which must be positive for real values of t. It was found that an initial guess too far from the optimum solution resulted in negative arguments of this radical at values of x less than 1.0, thus preventing even the initiation of a first iteration.

It was next decided to simplify the problem by taking only the real parts of all aerodynamic terms in the equations. The use of such purely static airloads will result in a slightly unrealistic situation, but the resulting problem does retain the essential features of the complete one, while reducing the number of unknowns by approximately half, from 25 to 13. At the same time, a corresponding solution was sought by assumed-mode methods, in the hope of starting with a small number of modes and adding thereto until an adequate approximation to the optimum solution was found. Each intermediate solution might provide an initial guess for most of the modal amplitudes in the next solution.

Under the chosen aerodynamic approximation, Eqs. (13)-(14) are completely real. Abandoning the state-vector description, one can reorganize them as two equations of motion, two Euler-Lagrange, or adjoint, equations, and a third Euler-Lagrange equation, the control equation:

$$
\begin{aligned}
&(ty'')'' - (\alpha_1 t + \alpha_2)\, y - (\beta_1 t + \beta_2)\theta = 0 \\
&(t\theta')' + (\gamma_1 t + \gamma_2)\, y + (\delta_1 t + \delta_2)\theta = 0 \\
&(t\lambda_r'')'' - (\alpha_1 t + \alpha_2)\, \lambda_r + (\gamma_1 t + \gamma_2)\, \lambda_s = 0 \\
&(t\lambda_s')' + (\delta_1 t + \delta_2)\, \lambda_s - (\beta_1 t + \beta_2)\lambda_r = 0 \\
&1 - \lambda_r'' y'' + \lambda_r (\alpha_1 y + \beta_1 \theta) + \lambda_s' \theta' - \lambda_s (\gamma_1 y + \delta_1 \theta) = 0
\end{aligned}
\tag{20}
$$

The boundary conditions are found from Eqs. (15)-(16), with some additional manipulation of Eqs. (20) to provide a specific boundary condition on t:

$$
\begin{aligned}
&y = y' = \theta = \lambda_r = \lambda_r' = \lambda_s = 0, \quad x = 0 \\
&t = y'' = \lambda_r'' = 0, \quad x = 1
\end{aligned}
\tag{21}
$$

Assumed modes that satisfy these boundary conditions are

$$y(x) = \sum_{n=1,3,\ldots}^{\infty} y_n \left(1 - \cos \frac{n\pi x}{2}\right)$$

$$\lambda_r(x) = \sum_{n=1,3,\ldots}^{\infty} \lambda_{rn} \left(1 - \cos \frac{n\pi x}{2}\right)$$

$$\theta(x) = \sum_{n=1}^{\infty} \theta_n \sin \frac{n\pi x}{2} \qquad (22)$$

$$\lambda_s(x) = \sum_{n=1}^{\infty} \lambda_{sn} \sin \frac{n\pi x}{2}$$

$$t(x) = \sum_{n=1}^{\infty} t_n \sin \frac{n\pi}{2}(1-x)$$

These series are substituted into Eqs. (20), and the Galerkin procedure is used to reduce the equations to nonlinear algebraic ones in the modal amplitudes. The first of Eqs. (20) is weighted with the modes for y, the second with the modes for θ, the third with the modes for λ_r, the fourth with the modes for λ_s, and the fifth with the modes for t (even though it no longer contains t explicitly).

Since the flutter speed and frequency for the reference wing are changed, they must be recomputed from the first two equations of Eqs. (20) with t = 1. A two-mode Galerkin procedure, with the two modes being the uncoupled fundamentals for a uniform beam in bending and torsion, yields a flutter frequency of 8.41 cps and a flutter speed of 270 fps for a wing with the physical properties given in Ref. 14. The flutter point is determined by modal coalescence, since the system is undamped. The same wing with out-of-phase aerodynamic loading included has a flutter frequency of 25.3 cps and a flutter speed of 333 fps, as calculated in Ref. 14. The system parameters for the simplified case are found

to be

$$\alpha_1 = 19.70, \quad \alpha_2 = -2.182, \quad \beta_1 = 9.2196,$$

$$\beta_2 = -22.89, \quad \gamma_1 = 0.1304, \quad \gamma_2 = 0.1897, \tag{23}$$

$$\delta_1 = 0.07410, \quad \delta_2 = 1.455$$

It is emphasized that these values are based on the assumption that virtually all of the mass of the wing is concentrated in the outer skin. The equations appropriate for sections with a fixed percentage of the total mass nonstructural in nature are quite simply derived from the foregoing, with the added restriction that the nonstructural mass must have the same sectional radius of gyration as the structural mass. For example, let η represent the fraction of the total mass at any section that is structurally effective. The stiffness terms in Eqs. (20) remain unchanged, but the inertial terms are altered. The equations for the new system are obtained from those for the old system by redefining the system parameters:

$$\begin{aligned}
\alpha_1' &= \eta\alpha_1, \quad \alpha_2' = (1-\eta)\alpha_1 + \alpha_2 \\
\beta_1' &= \eta\beta_1, \quad \beta_2' = (1-\eta)\beta_1 + \beta_2 \\
\gamma_1' &= \eta\gamma_1, \quad \gamma_2' = (1-\eta)\gamma_1 + \gamma_2 \\
\delta_1' &= \eta\delta_1, \quad \delta_2' = (1-\eta)\delta_1 + \delta_2
\end{aligned} \tag{24}$$

Calculations by the modal method were in fact carried out with 50% of the total mass effective structurally, in which case the system parameters are

$$\alpha_1 = 9.850, \quad \alpha_2 = 7.668, \quad \beta_1 = 4.610,$$

$$\beta_2 = -18.28, \quad \gamma_1 = 0.06518, \quad \gamma_2 = 0.2549, \tag{25}$$

$$\delta_1 = 0.03705, \quad \delta_2 = 1.492$$

There are two reasons for this alteration of the system. The obvious one is, of course, that it reflects a more realistic physical situation to have a certain portion of the total mass represent nonstructural material. However, it was also desired to avoid certain doubts about the existence of a physically meaningful solution. A study of the least-weight unswept wing with fixed pure-torsion flutter speed, as reported in Ref. 12, had shown that there were certain values of system parameters that gave a negative optimum thickness distribution. Apportioning the sectional mass as indicated above had proved to be effective in eliminating trouble with that former solution. In the present case this step was taken purely as a precautionary measure; no clear evidence as yet suggests that reasonable solutions do not exist, even when all of the mass is effective structurally and available for optimization.

The skin thickness distributions for two intermediate modal solutions are presented in Fig. 4. The number of modes assumed for each computation is indicated in the figure. The solid curve is the distribution for the least number of modes possible: one for y and λ_r, two for θ and λ_s, and one for t. The seven modal amplitudes obtained are the roots of a system of seven nonlinear algebraic equations, which were computed with a subroutine utilizing a least-squares algorithm due to Powell.[15] The dashed curve shows the distribution for a total of ten modes. As stated previously, an initial guess for seven of the ten modal amplitudes was obtained from the seven-mode solution.

The savings in total weight are also indicated alongside the plots. With η defined as before, the weight ratio furnished by Eq. (1) must be altered to read

$$m = \eta \int_0^1 t(x)\, dx + (1 - \eta) \tag{26}$$

Since $\eta = 0.5$ for the distributions of Fig. 4, the fractions given represent a saving of 92 % of the disposable mass. Clearly more modes are necessary to assure a closer approximation to the actual solution. Nevertheless, these numbers offer interesting, if slightly unrealistic, evidence of the possibilities of aeroelastic optimization.

IV. A DYNAMIC AEROELASTIC CONSTRAINT: PANEL FLUTTER

Consider now a panel, or plate-column, of infinite span as shown in Fig. 5. The exact solution for the flutter of such a panel with uniform thickness under the action of quasi-steady supersonic airforces is discussed in Ref. 16. A panel whose deflection is $\tilde{w}(x,\tau) = \frac{W(x,\tau)}{C}$ has its dimensionless equation of motion given by

$$\frac{\partial^4 \tilde{w}}{\partial x^4} + R_x \frac{\partial^2 \tilde{w}}{\partial x^2} + \lambda_0 \frac{\partial \tilde{w}}{\partial x} + \lambda_0 \left(\frac{M_\infty^2 - 2}{M_\infty^2 - 1}\right) \frac{C}{V} \frac{\partial \tilde{w}}{\partial \tau} + \frac{M_0 C^4}{D_0} \frac{\partial^2 \tilde{w}}{\partial \tau^2} = 0 \tag{27}$$

Under the assumption that the motion is simple harmonic, Eq. (27) reduces to the following:

$$\frac{\partial^4 w}{\partial x^4} + R_x \frac{\partial^2 w}{\partial x^2} + \lambda_0 \frac{\partial w}{\partial x} - \bar{K} w = 0 \tag{28}$$

Boundary conditions are taken as those appropriate for hinged supports:

$$w = w'' = 0, \quad x = 0, 1 \tag{29}$$

In a manner analogous to that discussed in Sect. III, the uniform panel will be used as the reference system.

Equation (28) for a panel of variable thickness, with neither in-plane loading nor aerodynamic damping, is altered to read

$$\frac{\partial^2}{\partial x^2}\left(\frac{D_p(x)}{D_0} \frac{\partial^2 w}{\partial x^2}\right) + \frac{2q_\infty C^3}{D_0 \sqrt{M_\infty^2 - 1}} \frac{\partial w}{\partial x} + \frac{M(x)}{M_0} \frac{M_0 C^4}{D_0} (i\omega)^2 w = 0 \tag{30}$$

The boundary conditions are

$$w = D_p w'' = 0, \quad x = 0, 1 \tag{31}$$

The uniform panel is a special case when $D_p(x) = D_0 = \text{constant}$.

The panel under study is a sandwich structure whose geometry and air speed are held constant at a given altitude, so that several simplifications of Eq. (30) can be made. It is easily seen that

$$\frac{D_p(x)}{D_0} = \frac{T(x)}{T_0} = t(x) \tag{32}$$

$$\lambda_0 = 2\, q_\infty C^3 / D_0 \sqrt{M_\infty^2 - 1} = \text{constant} \tag{33}$$

$$K_0 = \frac{M_0 C^2}{D_0}\, \omega_0^2 = \text{constant} \tag{34}$$

The flutter equation of motion then becomes

$$\frac{\partial^2}{\partial x^2}(tw'') + \lambda_0 w' - \frac{M_p(x)}{M_0} K_0 \left(\frac{\omega}{\omega_0}\right)^2 w = 0 \tag{35}$$

with boundary conditions

$$\begin{aligned} w = tw'' = 0, \quad x = 0 \\ w = tw'' = 0, \quad x = 1 \end{aligned} \tag{36}$$

To take into account the mass of the core, it is required that there be a fixed amount of distributed non-structural mass in the panel which remains at a fixed proportion of the total mass at every point on the panel. This relation between skin mass and non-structural mass is expressed as:

$$\frac{M(x)}{M_0} = \frac{M_{skin} + M_{fixed}}{M_0} = \eta t(x) + (1 - \eta) \tag{37}$$

The rationale for adding a nonstructural portion to the total mass is similar to that of Sect. III, although for this case no real proof has been discovered that a physically reasonable solution cannot be found for all possible values of η.

As before, the constraint equation, Eq. (35), is transformed into an equivalent set of first-order equations:

$$\begin{aligned} w' &= p \\ p' &= q/t \\ q' &= r \\ r' &= -\lambda_0 p + (\alpha^2 t + \beta^2) w \end{aligned} \tag{38}$$

where $\alpha^2 = K_0\, \eta\, (\omega/\omega_0)^2$, $\beta^2 = K_0(1-\eta)\,(\omega/\omega_0)^2$.

The Euler-Lagrange functional for the problem then becomes

$$F = t + \lambda_w(p - w') + \lambda_p(q/t - p') + \lambda_q(r - q') + \lambda_r[-r' - \lambda_0 p + (t\alpha^2 + \beta^2)w] \tag{39}$$

The Euler-Lagrange equations applied to this F yield

$$\begin{aligned} \lambda_p q/t^2 - \alpha^2 \lambda_r w &= 1 \\ \lambda_w' &= -(\alpha^2 t + \beta^2)\lambda_r \\ \lambda_p' &= -\lambda_w + \lambda_0 \lambda_r \\ \lambda_q' &= -\lambda_p/t \\ \lambda_r' &= -\lambda_q \end{aligned} \tag{40}$$

The boundary conditions are

$$w(0) = q(0) = \lambda_p(0) = \lambda_r(0) = 0$$
$$w(l) = q(l) = \lambda_p(l) = \lambda_r(l) = 0 \tag{41}$$

The control equation, here the first of Eqs. (40), may be used to find t(x) as a function of the other variables:

$$t(x) = \left[\frac{\lambda_p q}{1+\alpha^2 \lambda_r q}\right]^{1/2} \tag{42}$$

From Eq. (42) and Eqs. (41) t(x) is found to be zero at each end of the panel, so the requirement that $q = tw'' = 0$ at the ends is met without requiring that $w'' = 0$. As will be shown later, this point is important when one uses a modal representation for the variables in the problem.

Equations (38) and (40) can be reduced to three second order, non-linear differential equations:

$$1 - w''\lambda_r'' + \alpha^2 \lambda_r w = 0$$
$$(tw'')'' + \lambda_0 w' - (\alpha^2 t + \beta^2) w = 0 \tag{43}$$
$$(t\lambda_r'')'' - \lambda_0 \lambda_r' - (\alpha^2 t + \beta^2)\lambda_r = 0$$

The approach to the solution of this problem follows the same lines as that described in Sect. III, for many of the same reasons. At present it is being attempted to solve Eqs. (43) with assumed modes and Galerkin's method. The chosen modes are sine-cosine series that satisfy the boundary conditions for w, λ_r, and t:

$$t(x) = \sum_{n=1}^{\infty} t_n \sin n\pi x$$

$$w(x) = \sum_{m=1}^{\infty} \left\{ a_m \sin m\pi x + b_m \sin \pi x \sin m\pi x \right\} \tag{44}$$

$$\lambda_r(x) = \sum_{p=1}^{\infty} \left\{ c_p \sin p\pi x + d_p \sin \pi x \sin p\pi x \right\}$$

(Note in particular that terms with nonzero second derivative at the ends of the panel are included in the expressions for w and λ_r.) The roots of the nonlinear algebraic equations for the modal amplitudes are being computed with a subroutine based on a procedure due to Marquardt.[17] No meaningful results are available at the time of writing, although it is clear that the sensitivities are not so great that current difficulties cannot be overcome. A transition-matrix approach to Eqs. (39)-(41) has also not yet succeeded.

Another interesting aspect of the sandwich-panel optimization problem involves the question of uniqueness. Turner[9] has used a uniqueness assumption to prove that the optimum thickness distribution must be symmetrical about the panel midchord. His finite-element solutions tend to confirm this symmetry property, although finite-element numerical results do not provide absolute confirmation with respect to a differential-equation solution. On the other hand, if the solution is not unique--and uniqueness has by no means been proven in this case--Turner's proof is invalid. Aside from its other merits, a function-space solution to this problem offers the possibility of aiding greatly in resolving this question.

V. CONCLUDING REMARKS

In Ref. 12, two of the present authors discussed the physical significance that can be attached to the control equation when it is written in a certain way. For example, for the minimum-weight wing with fixed torsional divergence speed, as discussed in Sect. II, it can be interpreted as specifying a constant strain energy per unit thickness over the span of the wing. This constancy of energy density was proven to exist for a wide class of optimization problems with static conservative loads by Prager and Taylor (Ref. 7). It was generalized to include cases with nonconservative static loads in Ref. 12. For conservative dynamic optimization problems, such as the minimum-weight bar with a fixed natural frequency of free vibration, the kinetic energy is involved as well. Then the specific Lagrangian density is constant.[12, 18] When dynamic aeroelastic constraints are imposed, time-dependent nonconservative loads are involved, and Table I makes clear that the problem of physical interpretation may be more difficult. For pure-torsion flutter, the specific Lagrangian density associated with torsional straining is still constant. In the case of constraints on eigenvalues associated with panel flutter and bending-torsion flutter, however, the constant quantities have the form of a specific Lagrangian density but involve products of the physical variables and their adjoints. Whether or not these observations will advance from being merely interesting to furnishing genuinely useful procedures for the direct construction of control equations is, at present, merely a matter of speculation.

Although it would be premature to offer any final conclusions, it is possible to add some general remarks about the numerical methods that have been tried. Certainly the authors' early optimism[12] about the use of the transition-matrix procedure must be tempered somewhat. It is evident that this method's sensitivity to initially assumed boundary values, which has frequently accompanied its application to problems in optimal control,[11] will remain a major hurdle to be overcome. Experience gained in solving aeroelastic optimization problems will undoubtedly furnish certain insight, but it may in the long run prove most useful to adopt more sophisticated steepest-ascent or gradient methods. With them the possibility of obtaining physically impossible thickness distributions can be easily avoided.

Modal methods have already proved to be useful, especially when little a priori information about the optimum solution is avialable. However, finding the solutions of the resulting nonliner algebraic equations has not been a trivial matter. Experience shows that there are definitely right and wrong ways to increase the number of modes in going from one intermediate solution to another.

All of these observations can perhaps be summarized in a single one: a certain amount of analytical work must precede the application of any numerical technique, especially since there appears to be no single method that ensures success in every case. The research worker in aeroelastic optimization will have to equip his arsenal with a number of numerical methods, and he may have to try more than one on any given problem.

Finally, it is evident that much work remains to be done. For example, modal solutions for the optimum wing of Sect. III and the optimum panel of Sect. IV must be compared with transition-matrix or steepest-ascent solutions. The results available to date, although certainly incomplete, already suggest that the full extent of benefits of aeroelastic optimization in the design of more efficient aerospace structures has yet to be demonstrated.

REFERENCES

1. Lunn, R. E. et alii, "A Method for Calculating the Optimum Bending Stiffness Required to Provide a Specified Lift-Curve Slope for a Flexible, Sweptback Wing," Rept. No. NA-61-521, 1961, North American Aviation, Inc., Los Angeles, California.

2. Hodson, C. H., "Stiffness Requirements to Prevent Flutter of Moderate to High Aspect Ratio Surfaces," Rept. No. NA-64-745, Sept. 1964, North American Aviation, Inc., Los Angeles, California.

3. Hodson, C. H., "Estimation of Flutter Stiffness Requirements for Thin Low-Aspect-Ratio Wings," Rept. No. NA-65-794, Sept. 1965, North American Aviation, Inc., Los Angeles, California.

4. Schmit, L. A. and Thornton, W. A., "Synthesis of an Airfoil at Supersonic Mach Number," CR-144, Jan. 1965, NASA.

5. Niordson, F. I., "On the Optimum Design of a Vibrating Beam," Quarterly of Applied Mathematics, Vol. 23, No. 1, April 1965, pp. 47-53.

6. Taylor, J. E., "Minimum Mass Bar for Axial Vibration at Specified Natural Frequency," AIAA Journal, Vol. 5, No. 10, Oct. 1967, pp. 1911-1913.

7. Prager, W. and Taylor, J. E., "Problems of Optimal Structural Design," ASME Paper No. 67-WA/APM-29, 1967 (to appear in Journal of Applied Mechanics).

8. Turner, M. J. "Design of Minimum Mass Structures with Specified Natural Frequencies," AIAA Journal, Vol. 5, No. 3, March 1967, pp. 406-412.

9. Turner, M. J., "Optimization of Structures to Satisfy Flutter Requirements," Volume of Technical Papers on Structural Dynamics, AIAA Structural Dynamics and Aeroelasticity Specialist Conference and ASME/AIAA 10th Structures, Structural Dynamics, and Materials Conference, American Institute of Aeronautics and Astronautics, New York, 1969, pp. 1-8.

10. Halfman, R. L., Dynamics, Volume II: Systems, Variational Methods, and Relativity, Addison-Wesley, Reading, Mass., 1962, Chap. 10.

11. Bryson, A. E., Jr. and Ho, Y.-C., Applied Optimal Control, Blaisdell, Waltham, Mass., 1969.

12. Ashley, H. and McIntosh, S. C., Jr., "Application of Aeroelastic Constraints in Structural Optimization," Proceedings of the 12th International Congress of Applied Mechanics, Springer, Berlin, 1969 (to appear shortly).

13. Smilg, B. and Wasserman, L. S., "Application of Three-Dimensional Flutter Theory to Aircraft Structures," ACTR No. 4798, July 1942, Materiel Div., Army Air Corps.

14. Runyan, H. L. and Watkins, C. E., "Flutter of a Uniform Wing with an Arbitrarily Placed Mass According to a Differential-Equation Analysis and a Comparison with Experiment," Rept. 966, 1950, NACA.

15. Powell, M. J. D., "An Iterative Method for Finding Stationary Values of a Function of Several Variables," The Computer Journal, Vol. 5, 1962, pp. 147-151.

16. Bisplinghoff, R. L. and Ashley, H., Principles of Aeroelasticity, Wiley, New York, 1962, pp. 419-423.

17. Marquardt, D. W., "An Algorithm for Least-Squares Estimation of Nonlinear Parameters," SIAM Journal, Vol. 11, No. 2, June 1963, pp. 431-441.

18. McIntosh, S. C. and Eastep, F. E., "Design of Minimum-Mass Structures with Specified Stiffness Properties," AIAA Journal, Vol. 6, No. 5, May 1968, pp. 962-964.

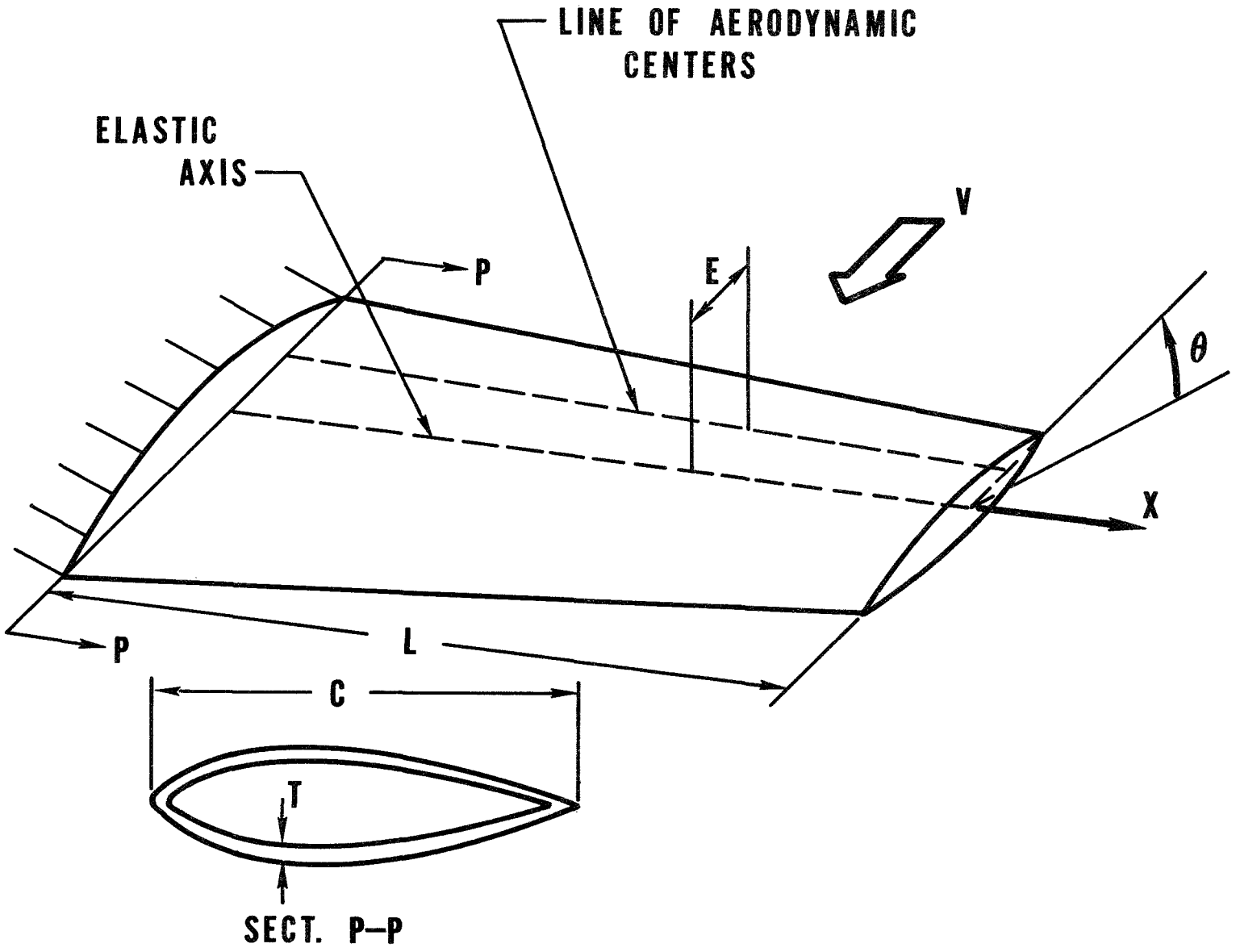

Figure 1. Unswept cantilever wing.

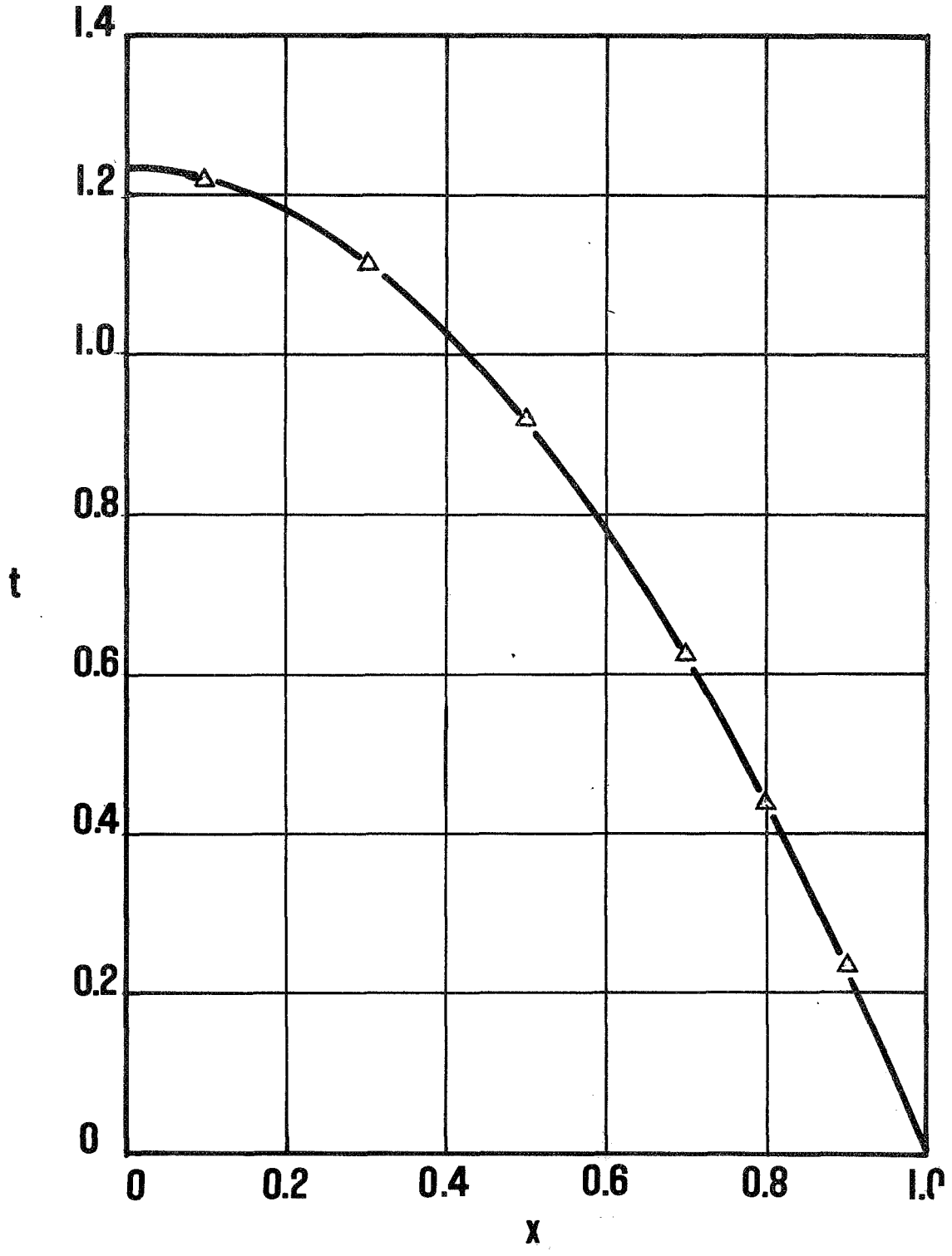

Figure 2. Optimum distribution of dimensionless skin thickness for the wing of Fig. 1 with rectangular planform. Analytically derived curve is compared with points calculated by means of a transition-matrix numerical method.

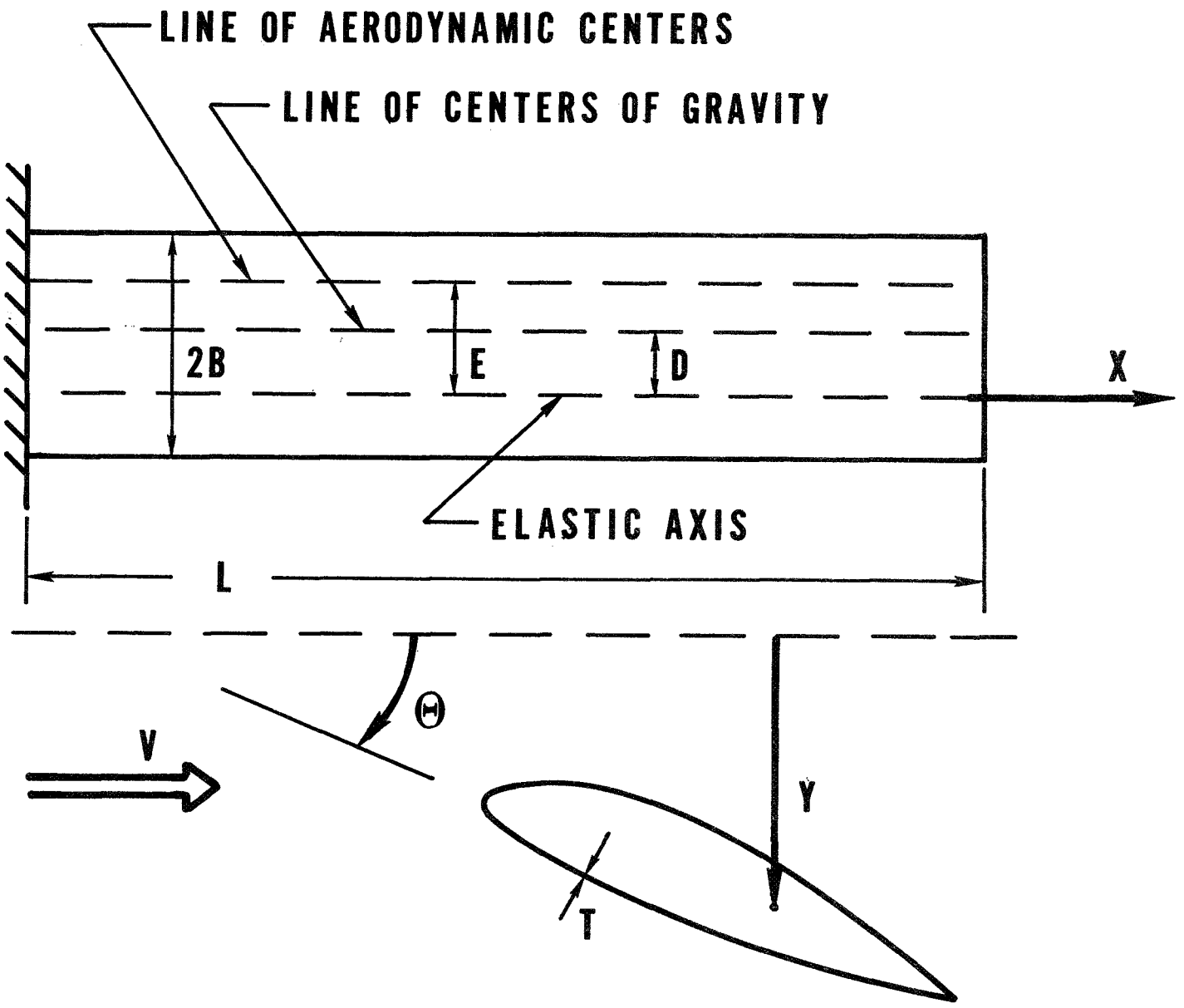

Figure 3. Rectangular cantilever wing, showing notation used for optimization with constant bending-torsion flutter eigenvalues.

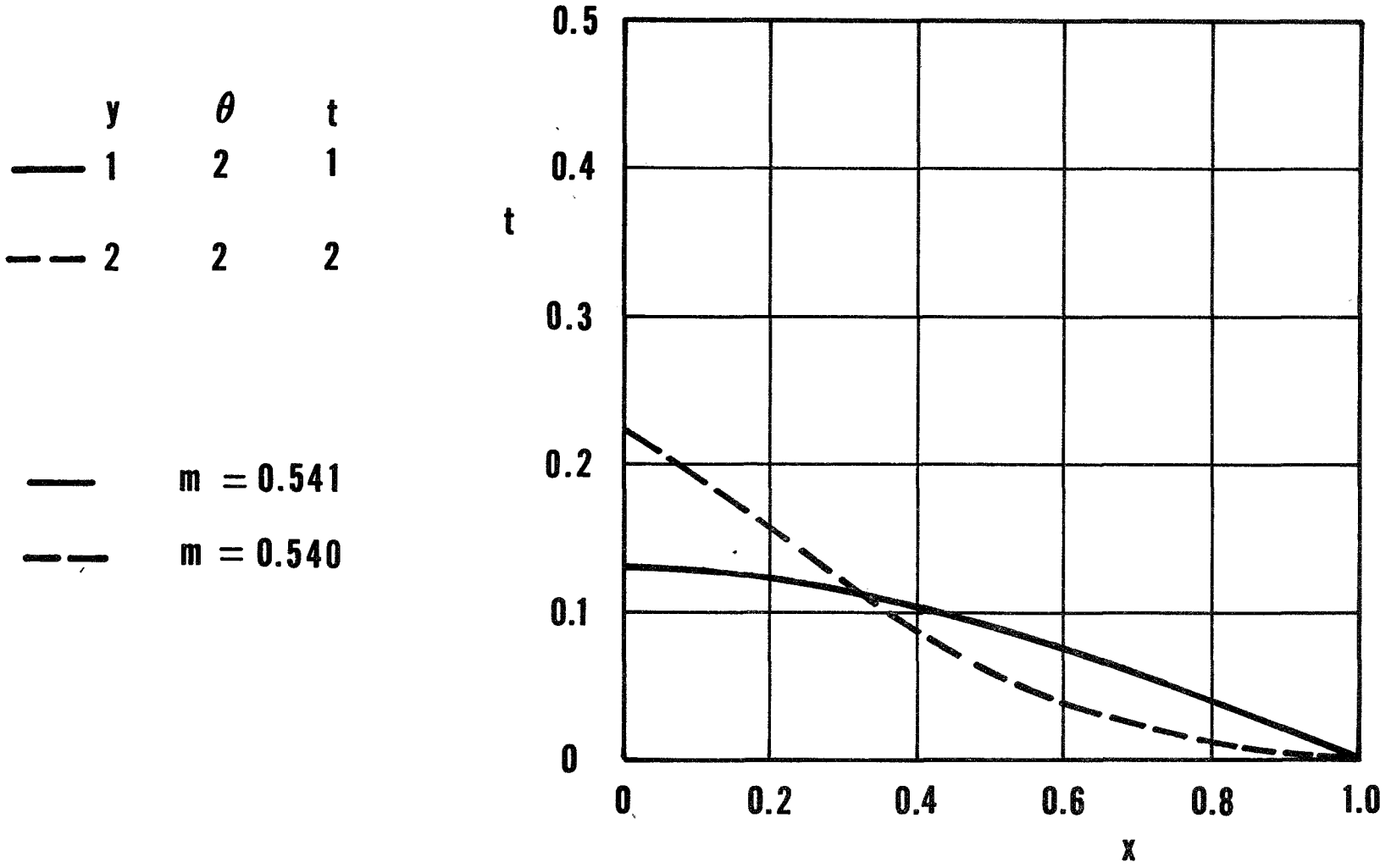

Figure 4. Intermediate modal solutions for dimensionless thickness distribution of wing of Fig. 3, plotted versus dimensionless spanwise coordinate. 50% of total section mass structurally effective; other system parameters given in Eqs. (25). Number of modes used and total mass savings are also indicated.

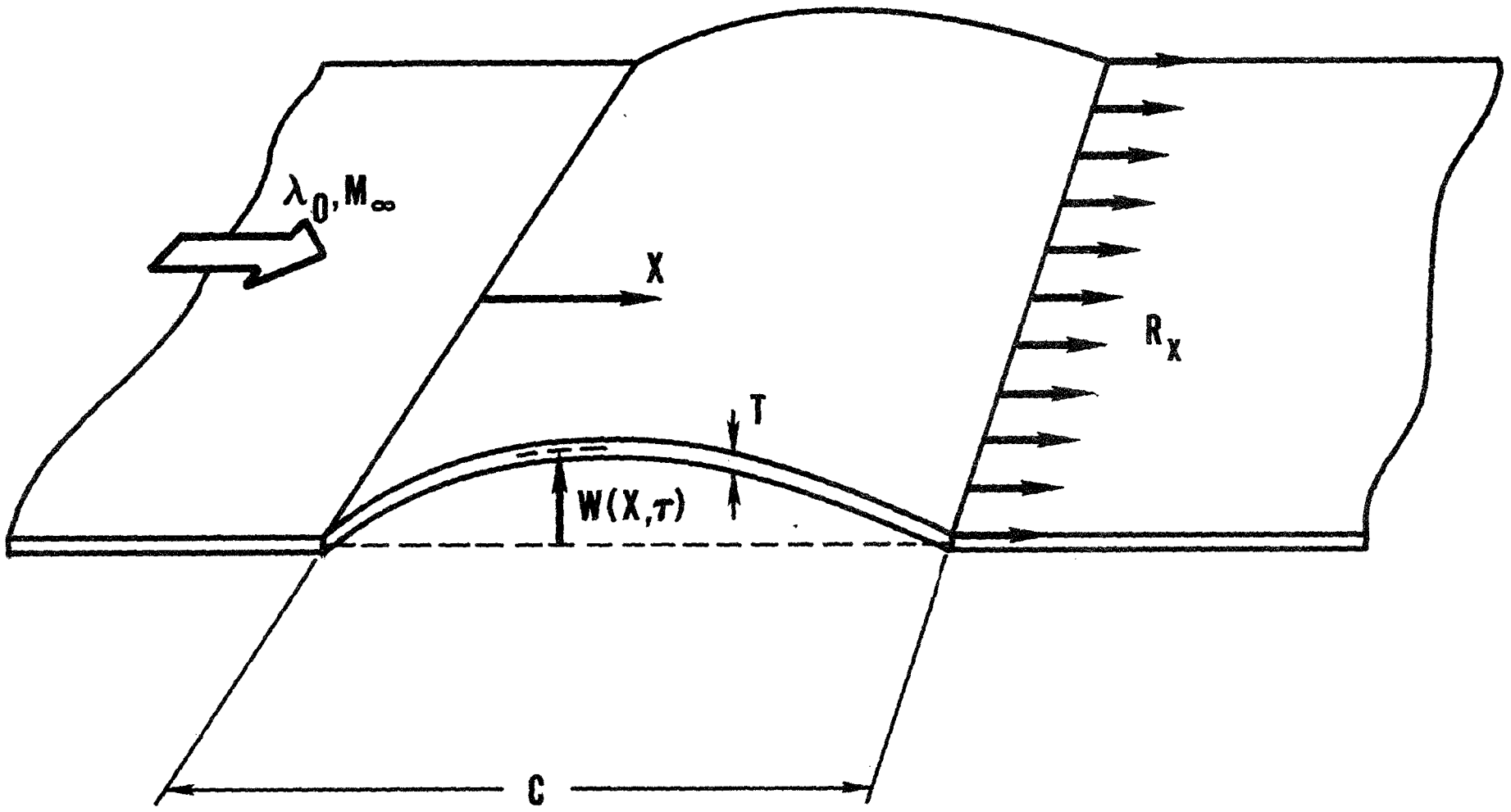

Figure 5. Panel (plate-column) of infinite span, showing notation used for optimization with constant flutter eigenvalues.

PHYSICAL PROBLEM	CONSTANT QUANTITY
TORSIONAL DIVERGENCE	$(\theta')^2$
PURE–TORSION FLUTTER	$(\theta')^2 - \delta_1 \theta^2$
PANEL FLUTTER	$w''\lambda_r'' - K_0\left(\frac{\omega}{\omega_0}\right)^2 \eta w \lambda_r$
BENDING – TORSION FLUTTER	$-\lambda_r'' w'' + \lambda_s' \theta'$ $+\lambda_r(\alpha_1 y + \beta_1 \theta)$ $-\lambda_s(\gamma_1 y + \delta_1 \theta)$

Table 1. Forms of control equation for various optimum systems.